Scientific Research Publishing

Materials Sciences and Applications, 2023, 14, 482-499
https://www.scirp.org/journal/msa
ISSN Online: 2153-1188
ISSN Print: 2153-117X

Evaluation of Reactive Oxygen Species (ROS) Generated on the Surface of Copper Using Chemiluminesence

Ken Hirota[1*], Hiroya Tanaka[2], Taika Maeda[2], Kazuhiko Tsukagoshi[2], Hiroshi Kawakami[3], Takashi Ozawa[4], Masahiko Wada[4]

[1]Research Center of Bio-Micro-Fluidic Science, Doshisha University, Kyoto, Japan
[2]Department of Chemical Engineering and Materials Science, Faculty of Science & Engineering, Doshisha University, Kyoto, Japan
[3]Graduate School of Engineering, College of Engineering, Osaka Metropolitan University, Osaka, Japan
[4]Japan Copper Development Association, Tokyo, Japan
Email: *khirota@mail.doshisha.ac.jp

How to cite this paper: Hirota, K., Tanaka, H., Maeda, T., Tsukagoshi, K., Kawakami, H., Ozawa, T. and Wada, M. (2023) Evaluation of Reactive Oxygen Species (ROS) Generated on the Surface of Copper Using Chemiluminesence. *Materials Sciences and Applications*, **14**, 482-499.
https://doi.org/10.4236/msa.2023.1410032

Received: August 26, 2023
Accepted: October 8, 2023
Published: October 11, 2023

Abstract

The antibacterial activity of copper is well-known from an ancient civilization, however, its biocidal mechanism has not been necessarily elucidated. Notwithstanding up to now, mainly 4 processes have been proposed. Among them, it is cleared that 4 kinds of reactive oxygen species (ROS): hydroxyl radical ·OH, hydrogen per oxide H_2O_2, superoxide anion $\cdot O_2^-$ and singlet oxygen $^1O_2$, play an important role for contact-killing of bacteria, viruses and fungi. In this paper, generation of ROS on the surfaces of copper plates heated from room temperature to 673 K for 4.2×10^2 s in air, was investigated using the chemiluminescence. ROS have been evaluated by selecting the most suitable scavengers, such as 2-propanol for ·OH, sodium pyruvate for H_2O_2, nitro blue tetrazolium for $\cdot O_2^-$, and sodium azide NaN_3 for $^1O_2$. At the same time the outermost surface of copper, on which thin film of cuprous oxide Cu_2O was first formed and then cupric oxide CuO was laminated on Cu_2O, was examined by thin-film XRD and TEM analysis to estimate the amounts and kinds of copper oxides. It was found that the most amounts of ROS were obtained for the 573 K-heated Cu plate and they were composed of ·OH, H_2O_2, and $\cdot O_2^-$.

Keywords

Copper, Microbial Activity, Reactive Oxygen Species, Chemiluminescence, Scavengers

1. Introduction

Copper and its alloys have been widely recognized from ancient to modern civilized societies as natural antibacterial materials [1], and they had been used as such as a water vessel, the building parts of shrine or temples, or a balustrade of bridge in Japan. Ancient civilizations utilized these antimicrobial properties long before the discovery of bacteria in modern civilization. Recently, the mechanism of antibacterial activity of copper and the related alloy has been much attracted again due to the worldwide disaster of Covid-19 [2]. Mainly 4 types of copper's antibacterial activities have been proposed [3] [4]; 1) bacteriolysis, *i.e.*, membrane breakdown; 2) membrane breakdown under stress; 3) DNA damages caused by reactive oxygen species (ROS) generated on the copper surface; 4) devolution and disaggregation of genome and or plasmid. These killing processes are multifaced with the main mechanism of bactericidal activity generated by ROS, which irreversibly brings damage of membranes and DNA chain in cell.

As far as oxygen concerned, there are 4 kinds of ROS [5], such as hydroxyl radical ·OH, hydrogen peroxide H_2O_2, superoxide anion $\cdot O_2^-$ and singlet oxygen $^1O_2$. Especially, ·OH reveals strong antibacterial activity due to its high reactivity which originates from high standard redox potential E_o = 2.38 V, the second highest followed by active fluorine E_o = 2.85 V [6]. Reactive oxygen species are generated on the surface of metal copper and metal oxides such as zinc and titanium oxides too. The present authors have been publishing some papers of the antibacterial activity of ZnO [7] [8] [9] anatase TiO_2 [10], which activity can be sustained even in a dark condition (*i.e.*, no sunlight). And further, a paper of anatase TiO_2 added Cu powders with improved antibiotic properties has been published recently [11]. Microscopically, the surface of metal copper is covered with very thin film of cuprous oxide Cu_2O and cupric oxide Cu_2O [12]. Therefore, ROS could be stated that its generation originates at the metal oxide surfaces [13].

Up to now, many ROS detection methods have been proposed [14]; electron spin resonance (ESR), fluorescence (FL), spectrophotometry, HPLC coupled with UV detection and chemiluminescence (CL). Among them, CL method has attracted much attention because of its unique advantages such as high sensitivity, instantaneity and simplicity of operation [15]. The detecting sensitivity much depends on the luminescence agents. Among emission agents, luminol is the most popular and has high sensitivity, therefore this agent is always used in a crime investigation. However, luminol has disadvantage, *i.e.*, this emission is limited by pH value of aqueous solution which contains antibacterial substance. It is reported that the best pH value is about 11.0 [16]. Furthermore, identification of ROS can be performed by selecting the suitable scavengers for each ROS in CL measurement. Many reports concerning about scavengers used in CL measurement have been published [17] [18]: 1). alcohol [19], mannitol, potassium formate, ascorbic acid, DMSO, and phthalhydrazide [20] [21] for hydroxyl radi-

cal ·OH, 2) riboflavin [22] [23], pyruvic acid [17] [24] for hydrogen peroxide H_2O_2, 3) ((2-Methyl-6-(4-methoxyphenyl) imidazo [1,2-a] pyrazin-3(7H)-one, $C_{14}H_{13}N_3O_2$, in simple terms as abbreviated, "MPEC" [25] and nitro blue tetrazolium (in simple terms, "nbt") [17] [18] [26] for superoxide anion $\cdot O_2^-$, and 4) 2,5-dimethylfuran, sodium azide "NaN_3" [17], MnTBAP (manganese(III)-tetrakis (4-benzoic acid) for singlet oxygen $^1O_2$. However, there are some features in each scavenger, for examples, its sensitivity, a combination of emission reagents, and pH dependence of efficiency. For examples, phthalhydrazide and riboflavin were incorrect deemed in this study, furthermore, n-butanol, which was reported to be the suitable scavenger for detecting hydroxyl radical, has been found to not suitable for CL method recently in our investigation. In our previous study, antibacterial activity of ZnO, anatase TiO_2 and Cu powders have been investigated to understand its mechanism and improve the antimicrobial properties, available even in a dark condition for the former two.

Purpose of this study is to inquire what kind of and how amount of ROS are generated on the surface of metal copper, using the combination of light emission reagent and scavengers in CL measurement, and by observation of the outermost surface by TEM and identification of crystalline phases by thin-film XRD.

2. Experimental Procedure

2.1. Preparation of Bulk Cu Plates

Oxygen-free copper (99.99% purity, C1020) plate, a square shape in size 25 × 25 × 1.0 mm^3 (Kikukawa Industry Co., Ltd, Tokyo, Japan), were used as starting material. These Cu plates, after wiping their surfaces with ethanol, were heated in air at 373, 473, 523, 573, 623, 673 K for 4.2×10^2 s; heat treatment was performed in quick heating and cooling.

2.2. Evaluation

2.2.1. Chemiluminescence (CL) Intensity Measurement and Evaluation of Reactive Oxygen Species (ROS)

Chemiluminescence (CL) of Cu plate in a 2.5×10^{-7} m^3 (0.25 mL) aqueous luminol solution with a concentration of 5.0×10^{-1} - 5.0×10^{-6} mol·m^{-3} (5.0×10^{-4} - 5.0×10^{-9} mol·L^{-1}) mixed with 4.0×10^{-6} m^3 (4.0 mL) carbonic acid buffer solution ($NaOH/NaHCO_3$, pH = 10.8 - 10.9) [27] was observed under dark conditions using a CL detector (CLA-FS3, Tohoku Electronic Industrial Co., Ltd., Sendai, Japan). After dropping the luminol solution in a 6.0×10^1 s' warming up of the detector, the intensity of CL was integrated between 6.1×10^1 - 6.0×10^2 s. The obtained summation of CL intensity for 5.4×10^2 s (9 min), SCL (9 min), which was calculated as follows: at first estimate summation of the background noise, SCL(BG), from 0 to 6.0×10^1 s, and then summarize the CL intensity from 6.1×10^1 to 6.0×10^2 s, SCL (total 9 min), finally, true SCL (9 min) was determined to be as true SCL (9 min) = SCL (total 9 min) – SCL (BG) × 9. This true

SCL (9 min), in simple terms, SCL (9 min) value was utilized to evaluate the amount of ROS generated from the surface of Cu plate.

Among 4 kind of ROS, such as ·OH, H_2O_2, $\cdot O_2^-$ and $^1O_2$, scavengers, 2-propanol ("2-pro", for ·OH, Nacalai Tesque Chemicals, Kyoto, Japan) [28] [29] [30], sodium pyruvate [17] ("s-pyr", for H_2O_2, Fuji-film Wako Pure Chemical Co., Ltd., Osaka, Japan), nitro blue tetrazolium [31] ("nbt", for $\cdot O_2^-$, Nacalai Tesque Chemicals) and sodium azide [17] (for short "NaN_3", for $^1O_2$, Fuji-film Wako Pure Chemical) were mainly used to determine which ROS is generated. At first these scavengers were solved in the buffer solution into the concentration 5.0×10^{-2} - 5.0×10^{-6} mol·L^{-1} and then obtained 0.25 mL or 0.50 mL scavenger solution were used. Each solution and a 4.0 mL pure buffer solution were mixed. CL measurement was performed as the same as CL intensity measurement, after a 6.0×10^1 s' warming up of the detector, the intensity of CL was integrated between 6.0×10^1 - 6.0×10^2 s. The amount of difference (D) for each ROS was evaluated using the equation of

D = SCL (9 min, without scavenger) − SCL (9 min, with scavenger) (1)

2.2.2. Physicochemical Property

Microstructural observation with a field emission-type scanning electron microscope (FE-SEM; SU8020, Hitachi High-Technologies Co., Ltd., Tokyo, Japan) and a transmission electron microscope (TEM, JEM-2100F, JEOL, Tokyo, Japan) equipped with the energy-dispersive X-ray spectroscopy (EDS, JED-2300T, JEOL) were performed. Then, the Cu samples were cut into a small specimen suitable for TEM observation using a focused ion beam (FIB, FB2200, Hitachi High-Technologies Co., Ltd.).

Thin-film X-ray diffraction (XRD; Smartlab, Rigaku, Tokyo, Japan) analysis using Cu*Ka* radiation (wavelength of 0.15418 nm) was utilized for identification of the crystalline phases and evaluation of lattice parameter of thin-film copper oxides, Cu_2O and CuO. Measuring conditions were as follows: accelerating electric voltage and current were 45 kV and 200 mA, respectively, scanning speed 1˚/min, scanning angle 2q: 20˚ - 80˚, angle of incidence 0.5˚ using a parallel X-ray beam. Under these conditions, the penetration depth of X-ray was estimated to be around 200 nm from the outermost surface [31]. Reference intensity ratio (RIR) analysis [32] was utilized to determine the mass % of Cu_2O and CuO.

3. Results and Discussion

Figure 1 shows a brief diagram explaining the flowchart of experimental results.

3.1. CL Intensity of Heated Cu Plates and Their Surface Morphology

As described at 2.2.2 in 2. Experimental procedure, chemiluminescence (CL) of Cu plates was measured using the luminol solution. Figure 2 shows dependence of CL intensity of as-received Cu plate on the concentration of luminol solution.

Based on the previous experimental data [11], their concentrations were varied from 5.0×10^{-4} to 5.0×10^{-9} mol/L (M). Except for extraordinary high CL intensity curve obtained using luminol's concentration of 5.0×10^{-4} M, the CL intensity was decreased gradually with decreasing luminol's concentration from 5.0×10^{-5} to 5.0×10^{-9} M. By considering the suitable intensity and linearity, the aqueous luminol solutions with concentration of 5.0×10^{-5} or 5.0×10^{-6} M were utilized in the present study. Then the Cu plates were rapidly heated for 4.2×10^{2} s and quenched in air to form copper thin-film oxides.

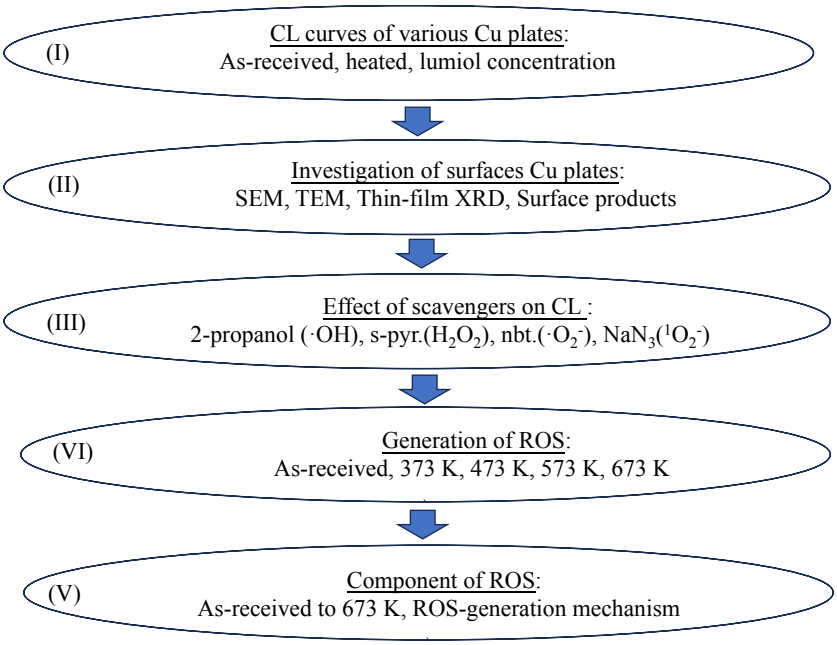

Figure 1. A brief diagram explaining the flowchart of experimental results.

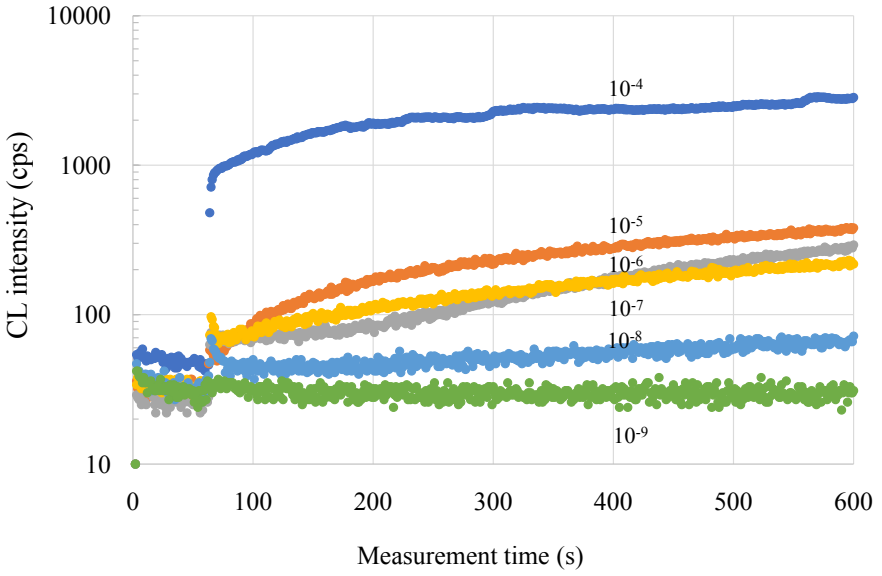

Figure 2. Dependence of CL intensity of as-obtained Cu plate on the concentration of luminol solution.

Figure 3 exhibits the CL curves of these heated Cu plates and the summation of CL intensity SCL (9 min) is displayed; here the luminol's concentration of 5.0×10^{-5} M was adopted. SCL (9 min) increased from 111.6×10^{3} count, *i.e.*, 111.6 k·count, to 736.6 k·count with increasing temperature up to 573 K and decreased rapidly to 48.5 k·count at 673 K, suggesting that SCL (9 min) depends much on the amount of copper oxides generated during the heat treatment in air and there might be the most suitable heating temperature. Luminol can emit light in pH value around 11.0 [16], then in order to eliminate pH effect we searched the light emission reagent which can perform in pH around 7. MPEC [25] is a reagent which can perform light emission in neutral pH, however, its intensity is very weak, so we used MPEC with the higher concentration than Luminol. Figure 4 shows SCL (9 min) of Cu plates prepared under various temperatures, which were determined using luminol (the concentration and the amount of instillation, 5.0×10^{-5} M and 2.50×10^{-7} m^3, 0.25 mL) and MPEC (5.0×10^{-1} M, 0.25 mL) under pH = 10.8 and 7.5 buffer solutions (4.0 mL), respectively. Both SCL (9 min) exhibited the highest value around 573 K; the best heating temperature is around 573 K. However, it was found that the top temperature sometimes shifted to the lower temperature, for example, 373 K or even room temperature, depending on the surface conditions of Cu plates as-received. Then, the surfaces of Cu plates heated at various temperatures were observed using an SEM under the magnification around 20,000 and compared. Figure 5 shows their images of various Cu plates; as-received (No. 1), and heated at 373 K (No. 2), 473 K (No. 3), 573 K (No. 4), and 673 K (No. 5) for 4.2×10^{2} s in air. Among the Cu plates from as-received to 473 K, little change has been recognized, however, 573 K-heated Cu plate showed the granular surface. Furthermore, at 673 K a small amount of needle-like granular were observed. As the highest SCL (9 min) value was attained on the Cu plate heated at 573 K, the outermost surfaces of Cu plates heated at 50 K lower and higher than the top temperature (573 K) were observed using the high-resolution TEM. Figure 6 displays the cross-section images of their outermost surfaces, in the top of each photograph upper left gray portion is bulk Cu, along to the right lower direction white thin film and black mass were observed on the surface of bulk Cu. Here, the magnifications of 1) 523 K and 2) 573 K are the same (see the scale bar of 100 nm), however, the right 3) 623 K is a little lower magnification (see the scale bar of 200 nm) because of the thick oxide film of Cu_2O, which will be described latter. Here we notice that the heating temperature increased from 523 to 573 K, "island-shaped, nub" film was first formed and grew along the base; "a hetero growth thin film (Cu oxide film on metal Cu)" was observed. This growth might be caused by "Volmer-Weber mode" [33] mechanism, that is, in the case that the surface tension of grown substance (Cu_2O) is larger than adhesion force and poor wettability between Cu_2O and Cu.

In the lower images with the higher magnification, the green line indicates the intensity of oxygen content along with a horizontal thin red line. As shown in Table 1, TEM observation gave the thickness of films about 40 to 100 nm for 1)

523 K and 2) 573 K samples, respectively, at 623 K-heated samples "non-uniform" layer. The former thickness values (40 and 100 nm) correspond well to those (40 and 100 nm) of Cu_2O formed on oxygen-free (<5 ppm) Cu heated at 473 K for 25 and 100 min in air, respectively, which is reported by M. Honkanen *et al.* [12]. Of course in the present study the heating conditions were much different: the temperature (523 K and 573 K) was much higher, and the soaking time (7 min) was very short. M. Honkanen *et al.* [12] also, described that below 473 K in air Cu_2O was first formed, and then above 473 K, Cu_2O changed into CuO by reacting with O.

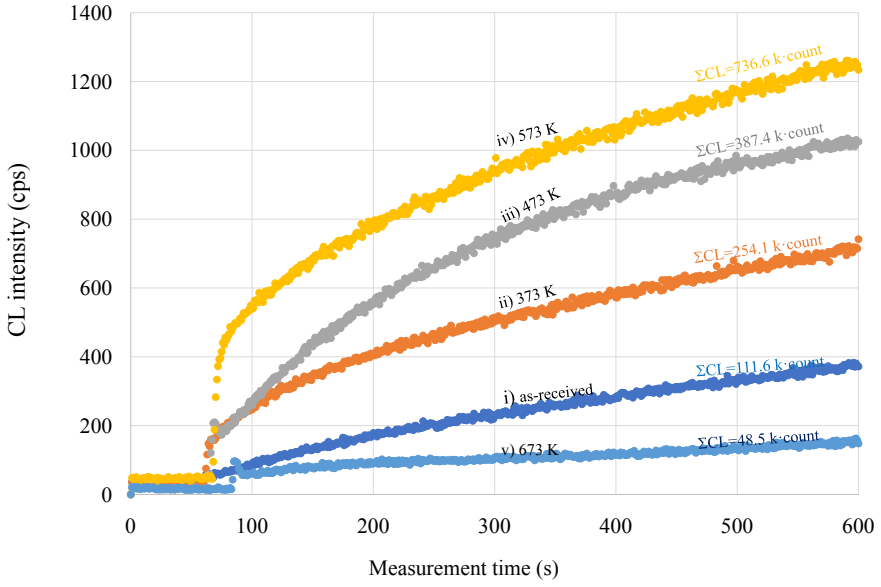

Figure 3. CL curves of Cu plates heated at various temperatures for 4.2×10^2 s in air.

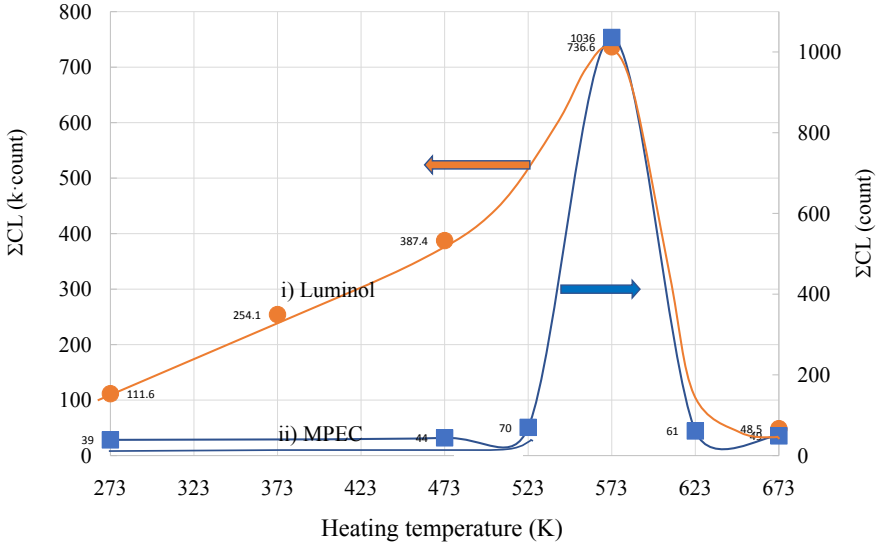

Figure 4. Summation of CL of Cu plates prepared under various heating temperatures, using Luminol (5.0×10^{-5} M, 0.25 mL) and MPEC (5.0×10^{-1} M, 0.25 mL) at pH = 10.8 and 7.5 buffer solutions (4.0 mL), respectively.

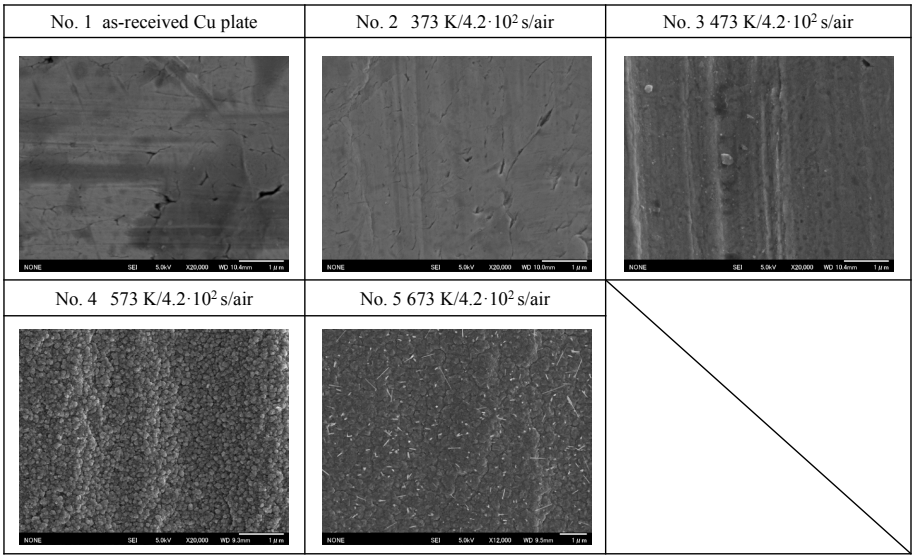

Figure 5. SEM photo images of the surfaces of Cu plates heated at various temperatures.

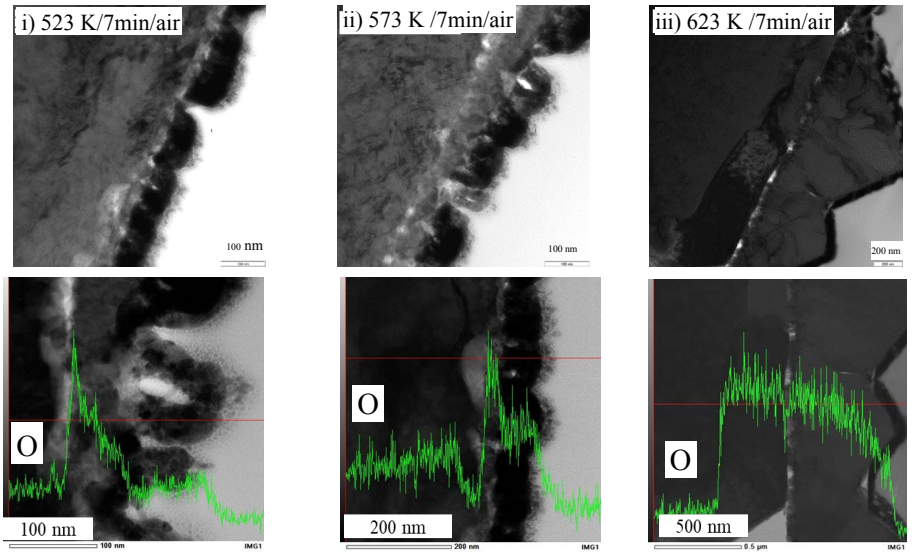

Figure 6. TEM images of the cross-section of surfaces of Cu plates heated at various temperatures for 4.2×10^2 s in air.

Table 1. Characteristics of oxide films formed on the surface of Cu plate heated at various temperatures.

(a) Characteristics of oxide films

Sample	Heating temperature (K) for 4.20 × 10^2 s in air	Thickness of films (nm) by TEM observation	Compositional ratio (at%) by EDX		Mass% of oxide films and their crystallite sizes (nm) by XRD*	
			Cu	O	Cu_2O	CuO
1)	523	around 40	90	10	6.0 (19.9)	0.25 (5.1)
2)	573	around 100	85	15	13.2 (17.4)	0.40 (5.6)
3)	623	non-uniform	82	18	22.6 (9.2)	6.05 (3.6)

(b) Lattice parameters of Cu_2O and CuO

	Cu_2O		CuO				
	a (nm)	V (nm^3)	a (nm)	b (nm)	c (nm)	b (°)	V (nm^3)
4) 523 K	0.42874	0.078810	0.46552	0.34117	0.51105	99.48	0.080057
5) 573 K	0.42721	0.077970	0.46485	0.34067	0.51031	99.48	0.079711
6) 623 K	0.42654	0.077605	0.46650	0.33977	0.51663	99.80	0.080693
	0.42520	0.078874	0.4649	0.34382	0.51870	98.64	0.081969
	Cu_2O PDF#1000063		CuO PDF#4105682				

*Thin film XRD was measured on the surface layers from the top to around 200 nm under.

By using the EDX analysis on thin films, the compositional ratios of Cu and O were determined. From the results of thin-film XRD analysis on Cu plates heated, which will be described in next **Figure 7**, the mass% of Cu_2O and CuO and their crystallite sizes were estimated (**Table 1(a)**). The content of Cu_2O was increased from 6.0 to 22.6 mass% gradually with increasing heating temperature up to 623 K, however, that of CuO increased suddenly from 0.40 to 6.05 mass% between 573 and 623 K. On the other hand, the crystallite size of Cu_2O reduced in size from 19.9 to 9.2 nm with increasing temperature, which may be reflected by the abrupt growth of CuO between 573 and 623 K. **Figure 7** shows the thin-film XRD patterns of Cu plates as-received (300 K) and heated at 473, 573, and 673 K for 4.2×10^2 s in air. XRD peaks of Cu_2O and CuO are not recognized on as-received Cu plate, however, heated at 473 K only a small Cu_2O peak appeared around 2q = 36.6˚, and at 573 K both Cu_2O and CuO peaks are observed. Furthermore, at 673 K many Cu oxides peaks were recognized. Based on these patterns, mass% of Cu_2O and CuO and crystallite sizes were estimated [32]. **Table 1(b)** shows the lattice parameters of cubic Cu_2O and monoclinic CuO formed on the Cu plate surfaces, with reported PDF data. At-a-glance, the lattice parameter a (042874 to 0.42654 nm) and unit volume V (0.078810 to 0.077605 nm^3) of Cu_2O phase are larger than those of the reported PDF data (a = 0.42520 nm and V = 0.07884 nm^3) and decreased gradually with increasing temperature, however, their changing degrees are very small. On the other hand, those of CuO phase except b values are almost the same with margin for error. **Figure 8** displays the Cu_2O and CuO contents (mass%) near the outmost surface of the Cu plates heated at various temperatures. Cu_2O gradually increased from 373 K and rapidly rose at 573 K, on the other hand, CuO showed little change up to around 573 K, which corresponding to the first Cu_2O formation at lower temperature than CuO on the Cu surface during heating in air. From this, temperature of 573 K might be the stage of sudden alternation, suggesting that copper oxides are active for generation of ROS.

3.2. CL Intensity of Heated Cu Plates with Scavenger

From the preliminary experiments, as we noticed that there must be the most suitable amount of each scavenger to suppress the generation of ROS, so investigation

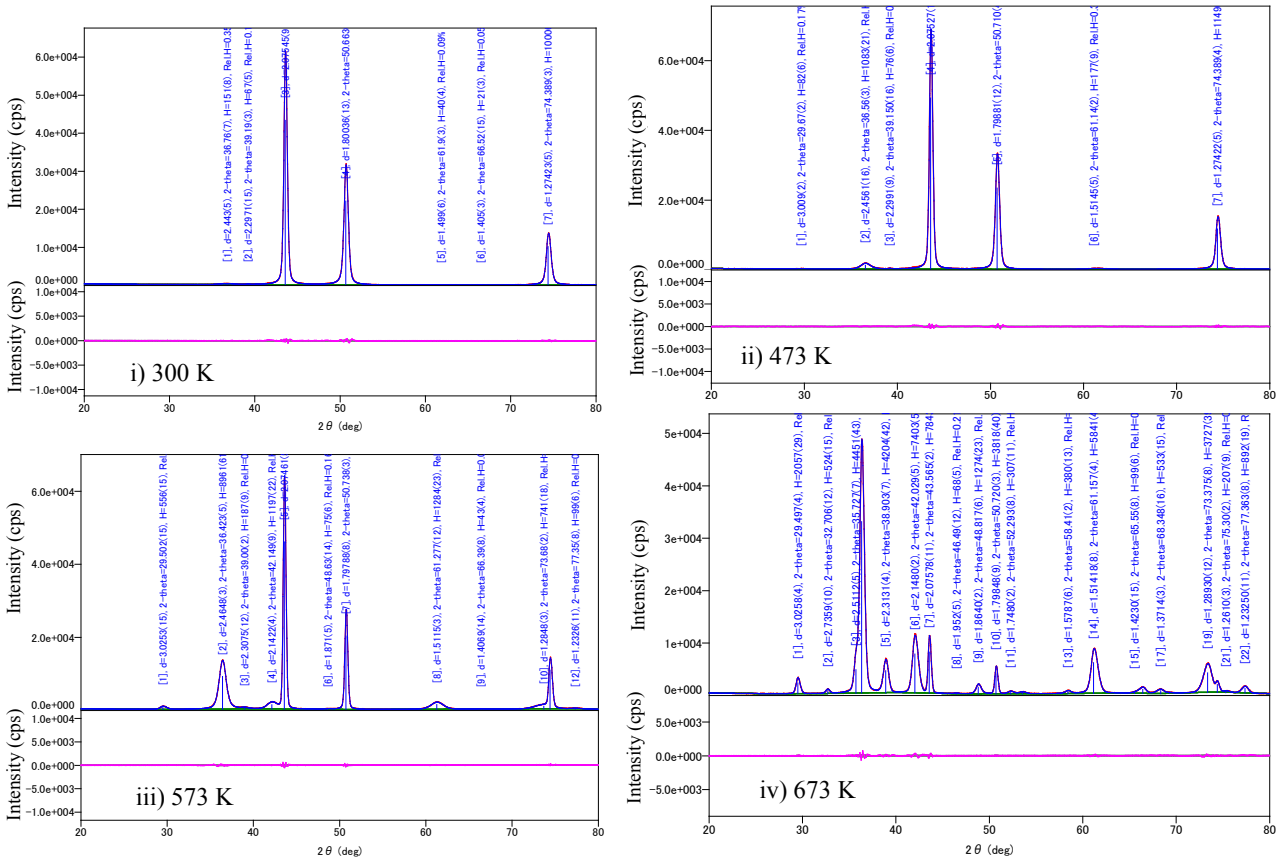

Figure 7. Thin-film XRD patterns of Cu plates heated at various temperatures for 4.2×10^2 s in air.

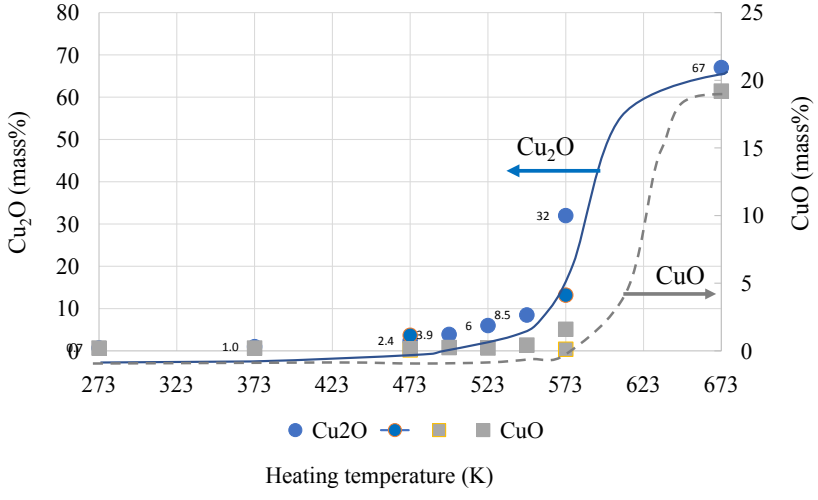

Figure 8. Contents of Cu_2O and CuO formed on the surface of Cu plates heated from room temperature to 673 K for 4.2×10^2 s in air.

of the relationship between SCL values and the amount of scavengers was performed. **Figure 9** displays the variations of SCL as a function of the amount of various scavengers. In this figure, the amount of luminol is constant (5.0×10^{-5} M, 0.25 mL) and, for example, the amount of instillation of nbt solution with the same concentration (5.0×10^{-5} M) as luminol was changed; the bottom point for

SCL is achieved around 0.50 mL, suggesting that the most suitable amount of nbt is 0.50 mL. And as the same manner, the most suitable amount of other scavengers were determined; for 2-propanol 0.25 mL, for s-pyr 0.50 mL and for NaN_3 0.50 mL tentatively. In the case of the last scavenger NaN_3, the 0.50 mL could reduce SCL value than that without scavenger and 1.0 mL (4 times higher mol ratio) addition might be too much.

Figure 10 summarized CL curves of as-received Cu plates added with the most suitable amounts of scavengers, using a constant amount of luminol (5.0×10^{-5} M, 0.25 mL) and the buffer solution (pH = 10.9, 5.0 mL); the values of SCL are also shown in this figure. Scavengers such as 2-propanol, nbt, s-pyr revealed the CL reduction, *i.e.*, among ROS which is formed on the Cu plate surface, hydroxyl radial ·OH, superoxide anion $\cdot O_2$ and hydrogen peroxide H_2O_2 were contained, however, singlet oxygen $^1O_2$ was not recognized. From the difference (D) between SCL values measured without and with scavengers, for example, D·SCL (2-propanol) = SCL (without 111.6) − SCL (with 53.1) = 58.5 k·count might be corresponding to the amount of ·OH. These amounts of each ROS formed on the heated Cu plates will be summarized later. **Figures 11-14** are the CL curves measured without and with each scavenger, using Cu plates heated at 373, 473, 573 and 673 K, respectively, for 4.2×10^2 s in air. In **Figure 13** and **Figure 14**, the scavenger's effect for singlet oxygen $^1O_2$ disappeared. Here, we have to mention that each scavenger cannot reduce only one ROS, *i.e.*, one scavenger might eliminate more than one ROS at the same time. Then, we calculate main ROS by normalizing. **Figure 15** is the summation of results showing the components of ROS formed on the heated Cu plates. At 573 K the highest amount of ROS was obtained and their main ROS were H_2O_2, $\cdot O_2^-$ and ·OH, however, we should consider the amount of H_2O_2 and ·OH are combined, because the formation of H_2O_2 is strongly related with the amount of ·OH due to the following equation of ·OH + ·OH = H_2O_2. Furthermore, even though some amounts of singlet oxygen $^1O_2$ are recognized at both 373 and 473 K, we might ignore its formation.

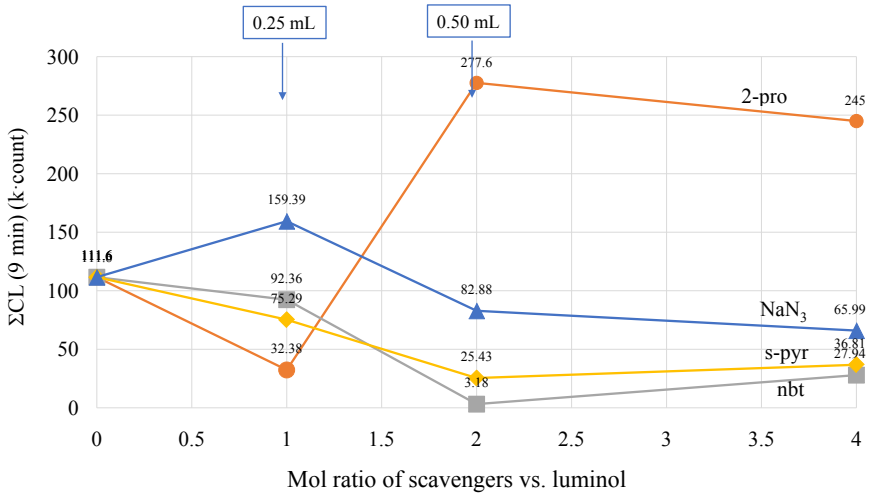

Figure 9. Summation of CL, SCL, of as-received Cu plate as a function of the mol ratio of scavengers vs. luminol.

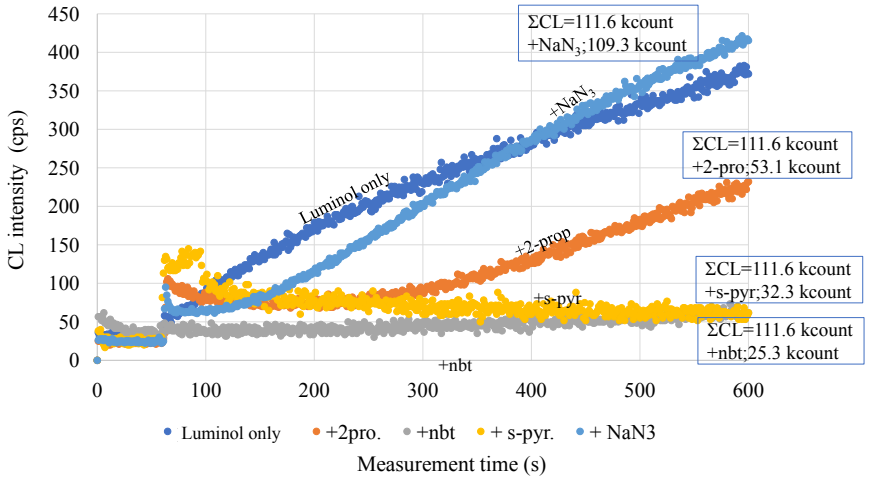

Figure 10. CL curves of as-obtained Cu plates measured using luminol and various scavengers.

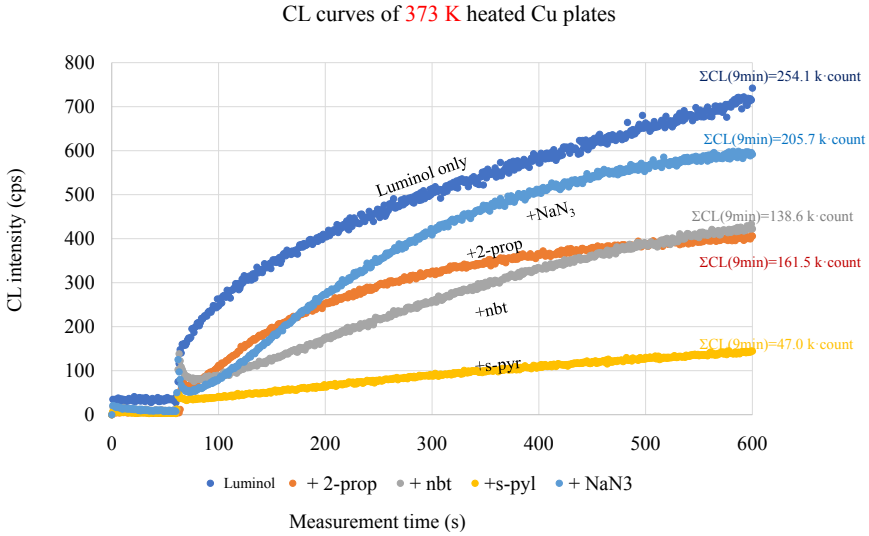

Figure 11. CL curves of 373 K-heated Cu plates measured using luminol and various scavengers.

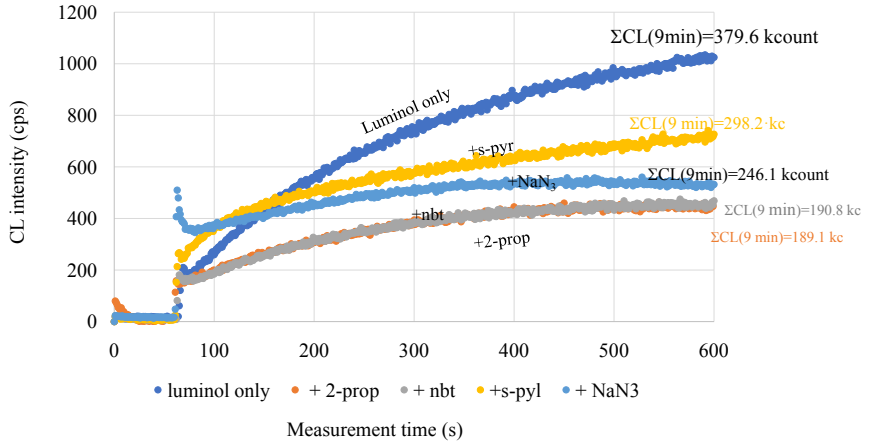

Figure 12. CL curves of 473 K-heated Cu plates measured using luminol and various scavengers.

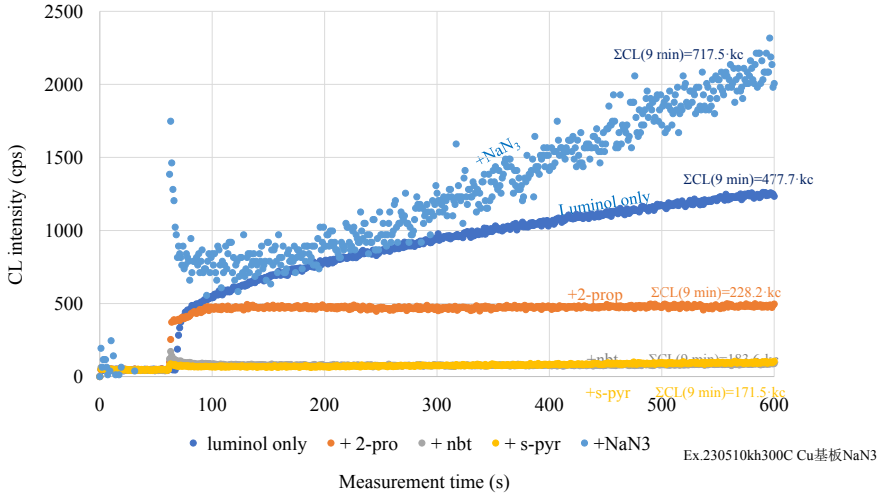

Figure 13. CL curves of Cu plate heated at 573 K for 4.2×10^2 s in air; luminol 5.0×10^{-5} M, 0.25 mL, buffer pH = 10.95, 5.0 mL, scavengers, such as, 0.25 mL 2-pro, 0.50 mL nbt and 0.50 mL s-pyr with the same concentration of 5.0×10^{-5} M were added.

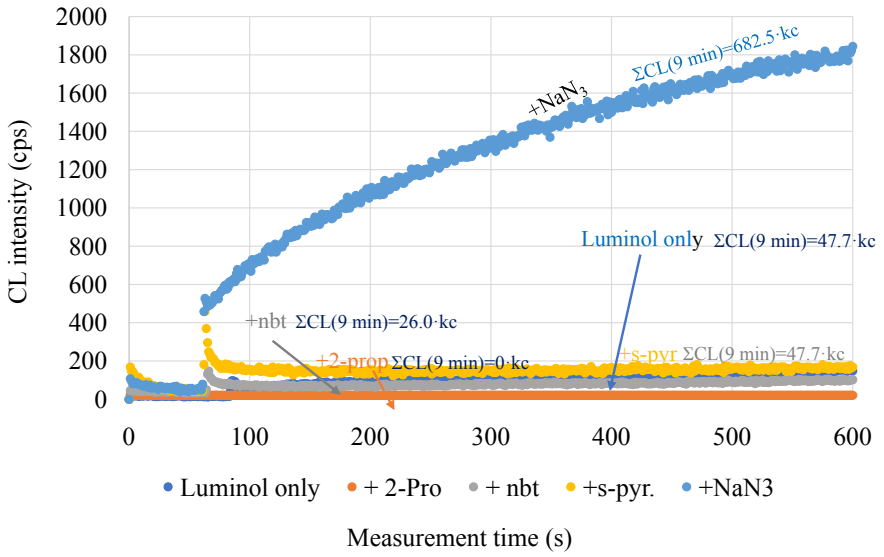

Figure 14. CL curves of Cu plate heated at 673 K for 4.2×10^2 s in air; luminol 5.0×10^{-5} M, 0.25 mL, buffer pH = 10.95, 5.0 mL, scavengers, such as, 0.25 mL 2-pro, 0.50 mL nbt and 0.50 mL s-pyr with the same concentration of 5.0×10^{-5} M were added.

Finally, the mechanism for generation of hydroxyl radical ·OH, hydrogen per oxide H_2O_2, and superoxide anion $\cdot O_2^-$ on the copper surface are proposed in **Figure 16**. As already described, a very fine and small amount of thin copper oxide films, Cu_2O and CuO are formed on the outermost surface in air. Cu bulk plate is drawn as a rectangular shape and placed in water or air. In the case of former, water contacts with air and the latter, air contains water vapor. Based on some chemical knowledge, *i.e.*, standard electrode potential E_0(Cu) = 0.34 V, SHE [standard hydrogen electrode]) [34], copper' stability in oxygen dissolved acidity or neutral aqueous solution, and a potential-pH diagram of Cu-H_2O at room temperature in air [35], Cu can be oxidized in the alkaline aqueous solution

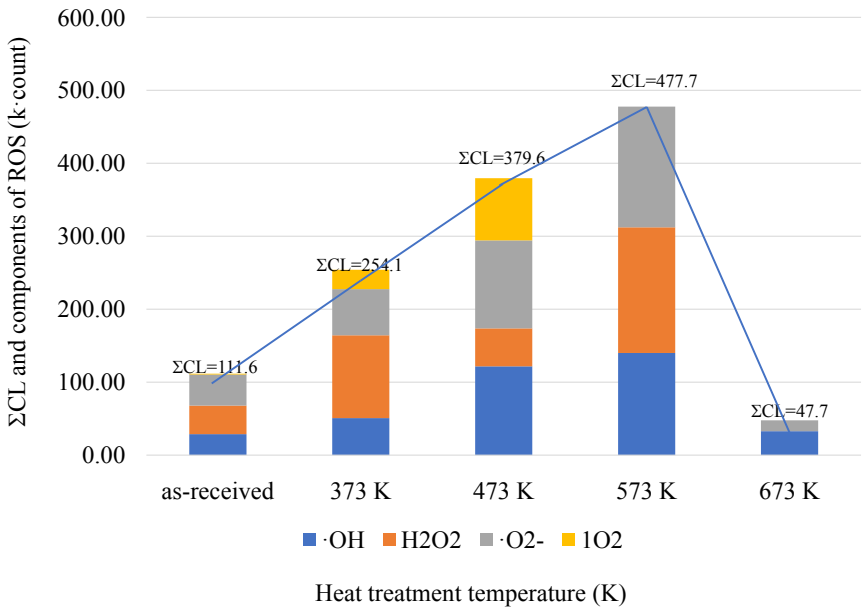

Figure 15. Summation of CL, SCL and components of ROS for Cu plates heated at various temperatures for 4.2×10^2 s in air.

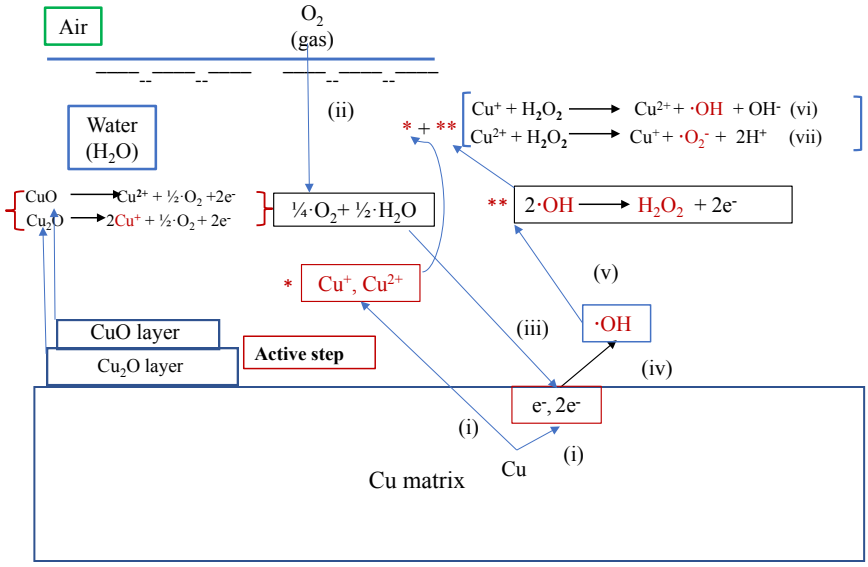

Figure 16. Schematic diagram for "Fenton reaction" to produce "ROS, ·OH, $\cdot O_2^-$" on the surface of Cu plate with thin copper oxides.

with pH = 7 - 14 by dissolved oxygen O_2; that is Cu --> Cu_2O or CuO. However, these products are supposed to be minute quantity due to a short reaction time for CL measurement of 6.0×10^2 s at 293 K. Therefore, in **Figure 16** (i) Cu in the bulk copper coelute into water at the surface; Cu --> $Cu^+ + e^-$ (or $Cu^{2+} + 2e^-$), (ii) O_2 in air dissolves into H_2O, (iii) and through the reaction ($1/4 \cdot O_2 + 1/2 \cdot H_2O$), it (OH) reacts with e^- (or $2e^-$) at metal surface, (iv) then ·OH is formed. Furthermore, (v) two ·OH changes into $H_2O_2 + 2e^-$. On the other hand, [* Cu^+ and Cu^{2+} in (i)] reacts with [H_2O_2 in (v)] into (vi) hydroxyl radical ·OH or (vii) superoxide

anion $\cdot O_2^-$. These (vi) and (vii) equations are called "Fenton Reaction" [13]. Here, at the first thin-film layer Cu_2O and the second layer CuO formed on the outermost surface of bulk Cu, as presented in upper side of **Figure 16**, ($2Cu^+ + 1/2 \cdot O_2 + 2e^-$) and ($Cu^{2+} + 1/2 \cdot O_2 + 2e^-$) are produced, respectively. These Cu^+ and Cu^{2+} react with H_2O_2, as presented by the equation (vi) and (vii); "Fenton Reaction" [13] takes place. It should be noted that these reactions tend to take place at "active step" of the edge place near islands of Cu_2O/CuO, not continuous thin-film.

4. Conclusion

By focusing on generation of reactive oxygen species (ROS) on the copper surface, the antibacterial activity of copper has been tried to explain. Especially, the change in ROS formed on the heated Cu plate was investigated: hydroxyl radical ·OH, hydrogen per oxide H_2O_2, and superoxide anion $\cdot O_2^- \cdot$ are the most of ROS. These data concerning about the components of ROS formed on the surface of heated Cu is reported for the first time using Chemiluminescence with the combination of luminol and scavengers. In addition, the generation mechanism of these three ROS on the outermost surface consisting of thin film Cu_2O, CuO layer and bulk Cu also is proposed.

Acknowledgements

The authors thank Ms. M. Toda of the Doshisha University Research Centre for Interfacial Phenomena, for FE-SEM and TEM observations of the samples.

Conflicts of Interest

The authors declare no conflicts of interest regarding the publication of this paper.

References

[1] Wikipedia, Free Encyclopedia. Antimicrobial Properties of Copper. https://en.wikipedia.org

[2] Govind, V., Bharadwaj, S., Ganesh, M.R.S., Vishnu, J., Shankar, K.V., Shankar, B. and Rajesh, R. (2021) Antiviral Properties of Copper and Its Alloys to Inactivate Covid-19 Virus: A Review. *BioMetals*, **34**, 1217-1235. https://doi.org/10.1007/s10534-021-00339-4

[3] Grass, G., Rensing, C. and Solioz, M. (2011) Metallic Copper as an Antimicrobial Surface. *Applied and Environmental Microbiology*, **77**, 1541-1547. https://doi.org/10.1128/AEM.02766-10

[4] Salah, I., Ivan, P. and Allan, P.E. (2021) Copper as an Antimicrobial Agent: Recent Advances. *RSC Advances*, **11**, 18179-18186. https://doi.org/10.1039/D1RA02149D

[5] Martinez, C.A., Nguyen, K.V., Ameer, F.S., Anker, J.N. and Brumaghim, J.L. (2017) Reactive Oxygen Species Generation by Copper(II) Oxide Nanoparticles Determined by DNA Damage Assays and ESR Spectroscopy. *Nanotoxicology*, **11**, 278-288. https://doi.org/10.1080/17435390.2017.1293750

[6] Srivishnu, K.S., Prasanthkumar, S. and Giribabu, L. (2021) Cu(II/I) Redox Couples: Potential Alternatives to Traditional Electrolytes for Dye-Sensitized Solar Cells. *Materials Advances*, **2**, 1229-1247. https://doi.org/10.1039/D0MA01023E

[7] Hirota, K., Sugimoto, M., Kato, M., Tsukagoshi, K., Tanigawa, T. and Sugimoto, H. (2010) Preparation of Zinc Oxide Ceramics with a Sustainable Antibacterial Activity under Dark Conditions. *Ceramics International*, **36**, 497-506. https://doi.org/10.1016/j.ceramint.2009.09.026

[8] Nguyen, T.M.P., Hirota, S., Suzuki, Y., Kato, M., Hirota, K., Taguchi, H., Yamada, H. and Tsukagoshi, K. (2018) Preparation of ZnO Powders with Strong Antibacterial Activity under Dark Conditions. *Japan Society of Powder and Powder Metallurgy*, **65**, 316-324. https://doi.org/10.2497/jjspm.65.316

[9] Nguyen, T.M.P., Hirota, K., Kato, M., Tsukagoshi, K., Yamada, H., Terabe, A. and Mizutani, H. (2019) Dependence of Antibacterial Activity of ZnO Powders on Their Physico-Chemical Properties. *Japan Society of Powder and Powder Metallurgy*, **9**, 431-441. https://doi.org/10.2497/jjspm.66.434

[10] Nguyen, T.M.P., Lemaitre, P., Kato, M., Hirota, K., Tsukagoshi, K., Yamada, H., Terabe, A., Mizutani, H. and Kanehira, S. (2021) Preparation of Anatase Titanium Dioxide Nanoparticle Powders Submitting Reactive Oxygen Species (ROS) under Dark Conditions. *Materials Science and Applications*, **12**, 89-110. https://doi.org/10.4236/msa.2021.122006

[11] Hirota, K., Jinzenji, A., Tsukagoshi, K., Taniguchi, Y., Kawakami, H., Ozawa, T., Wada, M. and Yuki, Y. (2023) Antibacterial Activity of Anatase TiO_2 Added Cu Powder. *Japan Society of Powder and Powder Metallurgy*, **70**, 121-131. https://doi.org/10.2497/jjspm.70.121

[12] Honkanen, M., Vippola, M. and Lepistö, T. (2008) Oxidation of Copper Alloys Studied by Analytical Transmission Electron Microscopy Cross-Sectional Specimens. *Journal of Materials Research*, **23**, 1350-1357. https://doi.org/10.1557/JMR.2008.0160

[13] Hans, M., Erbe, A., Mathews, S., Chen, Y., Solioz, M. and Mucklich, F. (2013) Role of Copper Oxides in Contact Killing of Bacteria. *Langmuir*, **29**, 16160-16166. https://doi.org/10.1021/la404091z

[14] Zhang, Y., Dai, M. and Yuan, Z. (2018) Methods for the Detection of Reactive Oxygen Species. *Analytical Methods*, **10**, 4625-4638. https://doi.org/10.1039/C8AY01339J

[15] Wanchao, Y. and Zhao, L. (2021) Chemiluminescence Detection of Reactive Oxygen Species Generation and Potential Environmental Application. *TrAC Trends in Analytical Chemistry*, **136**, Article ID: 116197. https://doi.org/10.1016/j.trac.2021.116197

[16] Oba, S. and Mukai, T. (2010) Mechanism and Condition of the Chemiluminescence of Luminol and Lucigenin. *Hiyoshi Review of Natural Science Keio University*, **48**, 31-57.

[17] For Example, Thermo Fisher Scientific Home. https://www.thermofisher.com

[18] Greenwald, R.A. (2017) Methods for Oxygen Radical Research. In: Greenwald, R.A., Ed., *CRC Handbook of Methods for Oxygen Radical Research*, CRC Press, Boca Raton, 177-179.

[19] Wang, L., Li, B., Dionysiou, D.D., Chen, B., Yang, J. and Li, J. (2022) Overlooked Formation of H_2O_2 during the Hydroxyl Radical-Scavenging Process When Using Alcohols as Scavengers. *Environmental Science and Technology*, **56**, 3386-3396.

https://doi.org/10.1021/acs.est.1c03796

[20] Miller, C.J., Rose, A.L. and Waite, T.D. (2011) Phthalhydrazide Chemiluminescence Method for Detection of Hydroyl Radical Production: Modifications and Adaptations for Use in Natural Systems. *Analytical Chemistry*, **83**, 261-268. https://doi.org/10.1021/ac1022748

[21] Pham, A.N., Xing, G., Miller, C.J. and Waite, T.D. (2013) Fenton-Like Copper Redox Chemistry Revisited: Hydrogen Peroxide and Superoxide Mediation of Copper-Catalyzed Oxidant Production. *Journal of Catalysis*, **30**, 54-64. https://doi.org/10.1016/j.jcat.2013.01.025

[22] Khan, S., Rayis, M.P., Rizvi, A., Alam, M.M., Rizvi, M. and Naseem, I. (2019) ROS Mediated Antibacterial Activity of Photo Illuminated Riboflavin: A Photodynamic Mechanism against Nosocomial Infections. *Toxicology Reports*, **6**, 136-142. https://doi.org/10.1016/j.toxrep.2019.01.003

[23] Ashoori, M. and Saedisomeolia, A. (2014) Riboflavin (Vitamin B2) and Oxidative Stress: A Review. *British Journal of Nutrition*, **111**, 1985-1991. https://doi.org/10.1017/S0007114514000178

[24] Kładna, A., Marchlewicz, M., Piechowska, T., Krukc, I. and Aboul-Eneind, H.Y. (2015) Reactivity of Pyruvic Acid and Its Derivatives towards Reactive Oxygen Species. *Luminescence*, **30**, 1153-1158. https://doi.org/10.1002/bio.2879

[25] ATTO.co.jp. https://www.atto.co.jp/reagents

[26] Wang, L., Liu, S., Zheng, Z., Pi, Z., Song, F. and Liu, Z. (2015) Rapid Assay for Testing Superoxide Anion Radical Scavenging Activities to Natural Pigments by Ultra-High Performance Liquid Chromatography-Diode-Array Detection Method. *Analytical Methods*, **7**, 1535-1542. https://doi.org/10.1039/C4AY02690J

[27] The Chemical Society of Japan (2021) Handbook of Chemistry: Pure Chemistry. 6th Edition, Maruzen-Publishing, Tokyo.

[28] Kozmér, Z., Takács, E., Wojnárovits, L., Alapi, T., Hernádi, K. and Dombi, A. (2016) The Influence of Radical Transfer and Scavenger Materials in Various Concentrations on the Gamma Radiolysis of Phenol. *Radiation Physics and Chemistry*, **124**, 52-57. https://doi.org/10.1016/j.radphyschem.2015.12.011

[29] Reisz, E., Clemens, V.S., Tekle-Röttering, A., Naumov, S., Schmidt, W. and Schmidt, T.C. (2018) Reaction of 2-Propanol with Ozone in Aqueous Media. *Water Research*, **128**, 171-182. https://doi.org/10.1016/j.watres.2017.10.035

[30] Kormali, P., Triantis, T., Dimotikali, D., Hiskia, A. and Papaconstantinou, E. (2006) On the Photooxidative Behavior of TiO_2 and $PW_{12}O_{40}^{3-}$: OH Radicals versus Holes. *Applied Catalysis B*: *Environmental*, **68**, 139-146. https://doi.org/10.1016/j.apcatb.2006.07.024

[31] Wojcieszak, D., Domaradzki, J., Kaczmarek, D. and Michalec, B. (2008) Characterization of Thin Films Based on TiO_2 by XRD, AFM and XPS Measurements. 2008 *International Students and Young Scientists Workshop—Photonics and Microsystems*, Wroclaw-Szklarska Poreba, 20-22 June 2008, 96-99. https://doi.org/10.1109/STYSW.2008.5164154

[32] Quantitative Analysis, Reference Intensity Ratio (RIR), ICDD (International Center of Diffraction Data).

[33] Meissner, C., Ploch, S. and Kneissl, M. (2009) Volmer-Weber Growth Mode of InN Quantum Dots on GaN by MOVPE. *Physica Status Solidi C*, **6**, S545-S548. https://doi.org/10.1002/pssc.200880872

[34] Gregory, J. (2020) Standard and Reversible Hydrogen Electrodes: Theory, Design,

Operation, and Applications. *ACS Catalysis*, **10**, 8409-8417.
https://doi.org/10.1021/acscatal.0c02046

[35] Meshram, P., Prakash, U., Bhagat, L., Abhilash, Zhao, H. and Hulleebush, E.D. (2020) Processing of Waste Copper Converter Slag Using Organic Acids for Extraction of Copper, Nickel, and Cobalt. *Minerals*, **10**, Article No. 290.
https://doi.org/10.3390/min10030290